

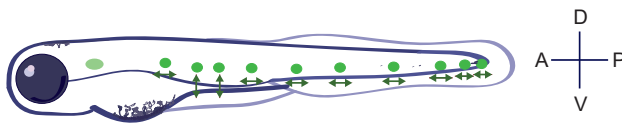
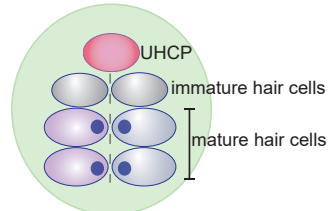
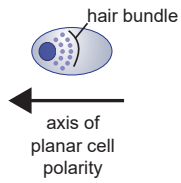
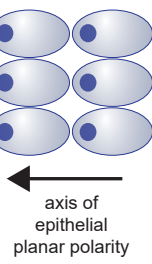
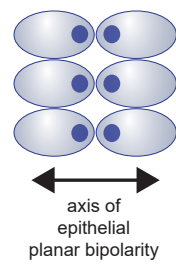
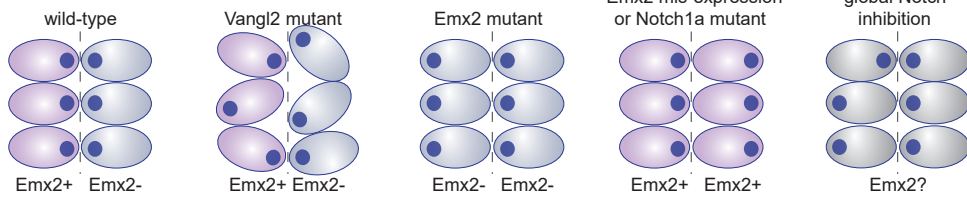
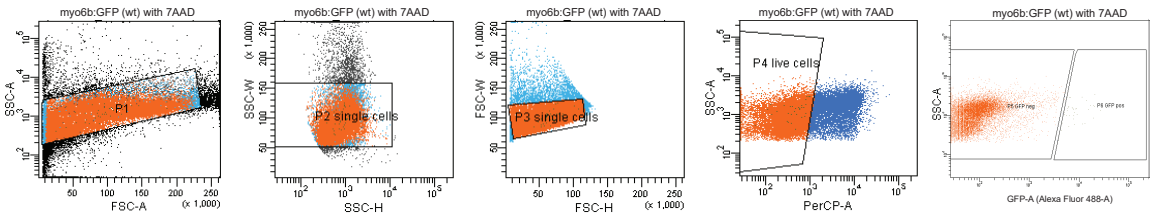
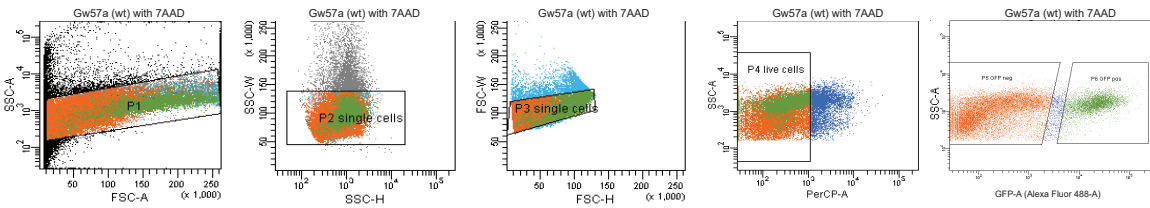
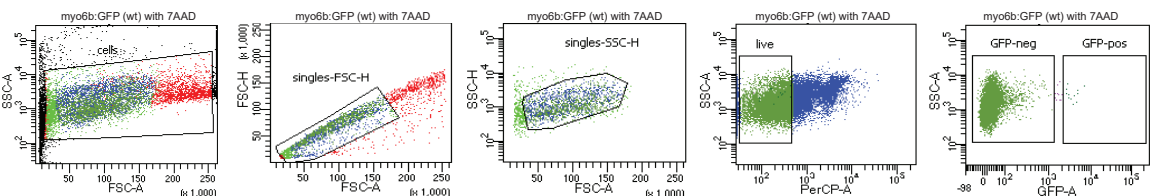
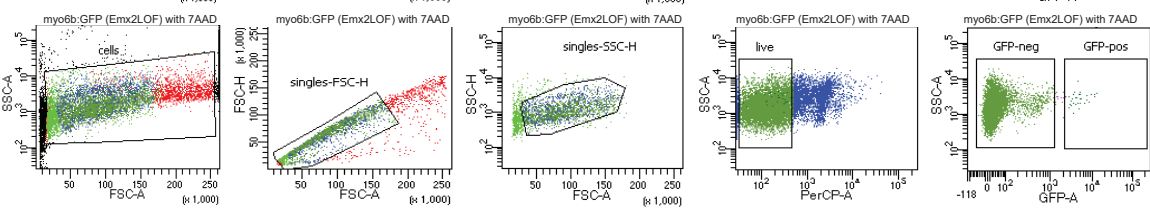
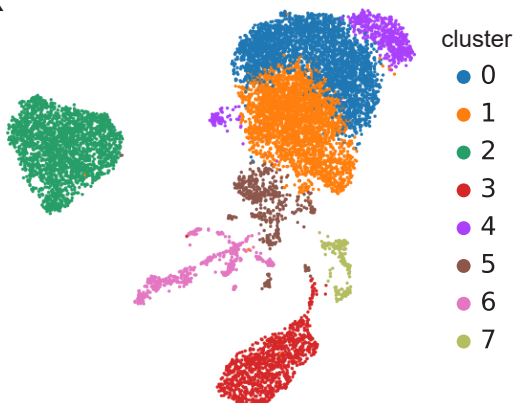
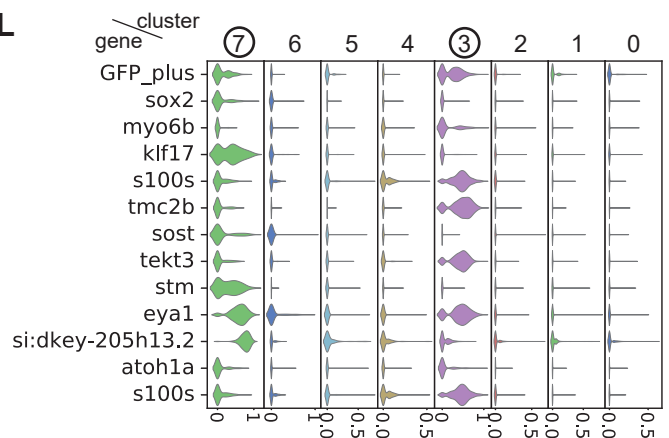
**Current Biology, Volume 30**

## **Supplemental Information**

### **Epithelial Planar Bipolarity Emerges**

#### **from Notch-Mediated Asymmetric Inhibition of Emx2**

**Eva L. Kozak, Subarna Palit, Jerónimo R. Miranda-Rodríguez, Aleksandar Janjic, Anika Böttcher, Heiko Lickert, Wolfgang Enard, Fabian J. Theis, and Hernán López-Schier**

**A****B****C****D****E****F****G****H****I****J****K****L**

**Figure S1. Schematic representation of planar polarity and cell isolation and selection process. Related to Figure 1.**

(A) A larval zebrafish showing the localization of horizontal and vertical neuromasts, whose axes of planar polarity are shown by double-headed green arrows. (B) A horizontal neuromast, showing the non-sensory epithelium in green, a unipotent hair cell progenitor (UHCP) in pink, a pair of immature hair cells in grey, and plane-polarized mature hair cells in magenta and blue. The transversal dashed line depicts a dorsoventral midline that coincides with the LPR in the organ. (C) A typical hair cell apex, with an eccentric kinocilium and the horseshoe-shaped hair bundle. A black arrow indicates the cell's axis and direction of planar polarity, which conventionally originates opposite to the kinocilium. (D) Several hair cells with coherent orientation along the epithelial planar-polarity axis. (E) Several hair cells with opposing orientation to exemplify epithelial planar bipolarity (shown by a double-headed black arrow). (F) Pairs of hair cells in wild type, and in various defective configurations indicated above each scheme. Magenta hair cells express *Emx2*, whereas blue cells do not. In this scheme, the expression status of *Emx2* in grey cells is unknown. The transversal dashed line depicts the dorsoventral midline. (G) FACS plots showing the isolation of single live GFP-labeled cells from *myo6b:EGFP* transgenic larvae (hair cells sample, sequenced by 10x Genomics in the next step). (H) FACS plots showing the isolation of single live GFP-labeled cells from *Gw57a* transgenic larvae (support cells sample, sequenced by 10x Genomics in the next step). (I) FACS plots showing the isolation of single live EGFP-labeled cells from wt *myo6b:EGFP* transgenic larvae (wt hair cells sample, sequenced by mcSCRBseq in the next step). (J) FACS plots showing the isolation of single live EGFP-labeled cells from *Emx2*-mutant *myo6b:EGFP* transgenic larvae (*Emx2*<sup>-/-</sup> hair cells sample, sequenced by mcSCRBseq in the next step). (K) UMAP plot showing the clustering of 10,431 single cells from combining hair cells and support cells samples (sequenced by 10x Genomics), also including the GFP-negative cells, which were added to the sample as control of sorting specificity. Clusters 3 and 7 consist of neuromast cells as identified by marker genes expression shown in panel D. (L) Violin plots showing the expression of selected neuromast marker genes and genes with high expression in neuromasts in each cluster. Neuromast marker genes were detected in clusters 3 and 7. These clusters were selected for more refined analysis.

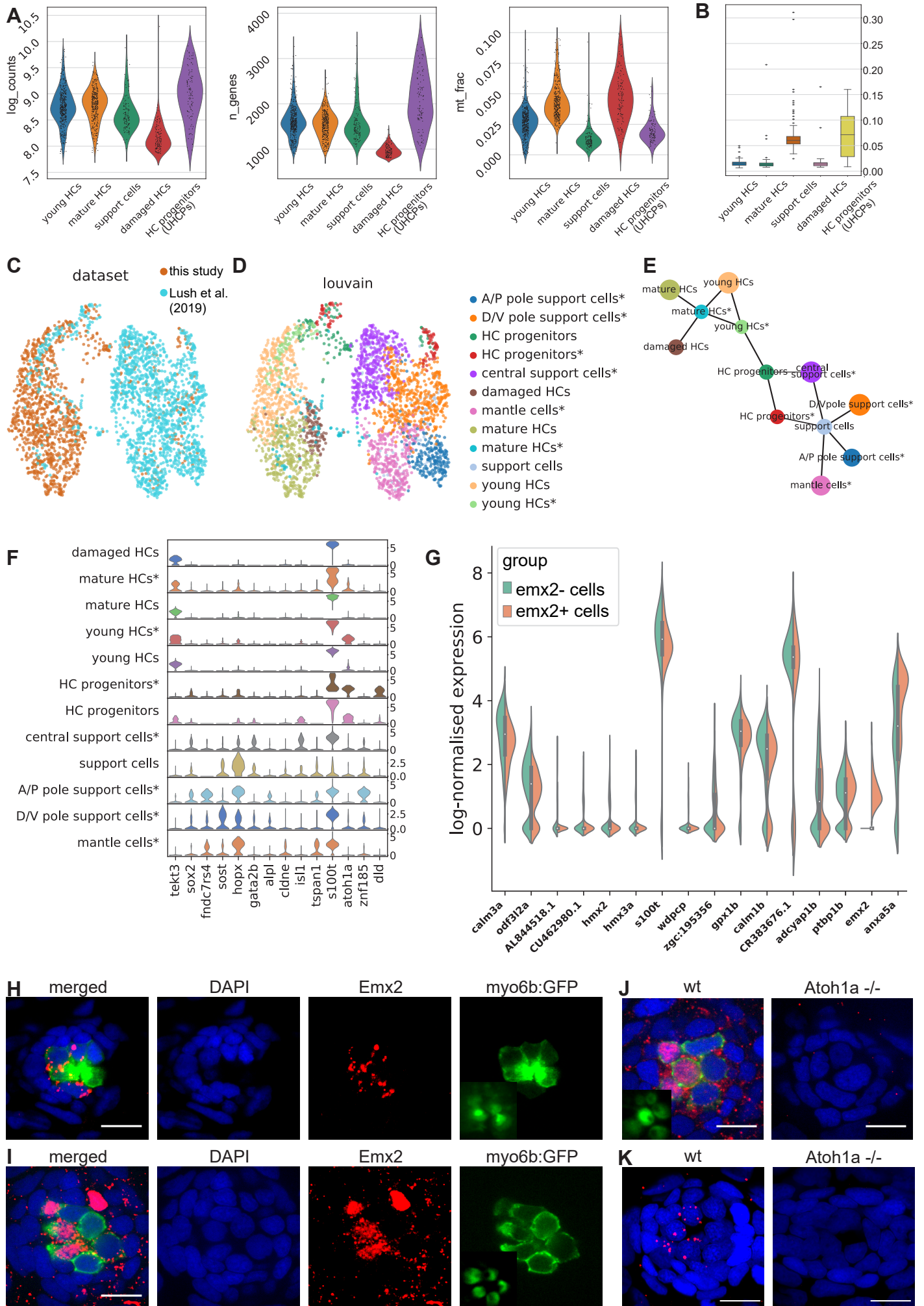
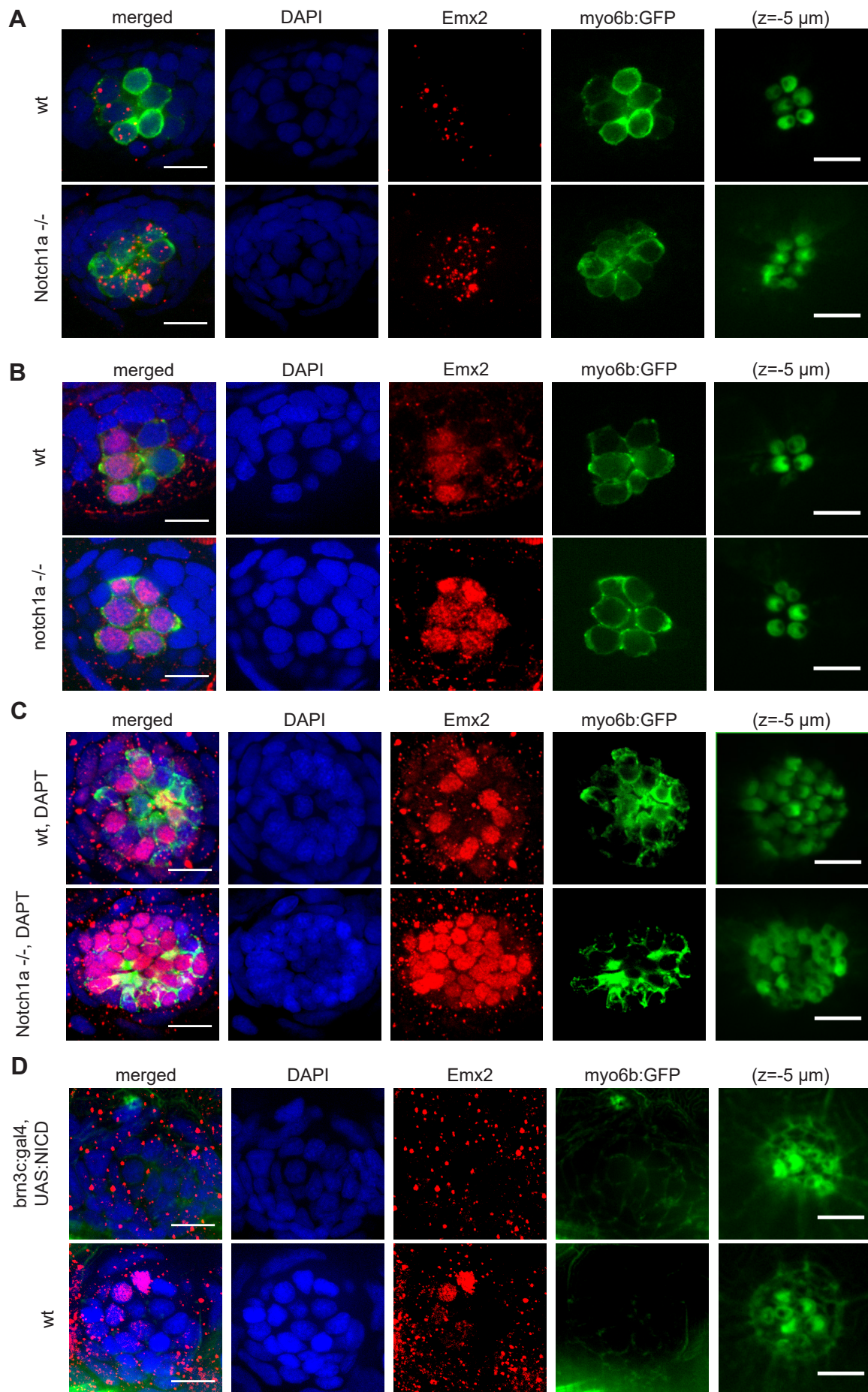


**Figure S2. Single-cell transcriptional analysis of neuromast hair cells. Related to Figure 1 and Table S1.**

(A) Violin plots showing the distribution of count depth, number of detected genes and the fraction of reads from mitochondrial genes (mt-) in neuromast cells after second-level clustering. (B) Distribution of doublet scores across groups after second-level clustering after filtering out technical artifacts of cell doublets. (C) UMAP plot showing the clustering of single cells from this study and the dataset published by Lush et al. (2019)[25]. (D) Annotated clusters of single cells from this study and Lush et al. (2019)[25], the latter marked with stars (\*). (E) PAGA plot showing the annotated clusters of single cells from this study and Lush et al. (2019)[25], the latter marked with stars (\*). The weight of the edges corresponds to stronger links between clusters, which could be interpreted as transcriptional similarity between states. The size of the dots correlates with the fraction of cells within each cluster. (F) Violin plot showing the expression of selected genes in the clusters of single cells from this study and Lush et al. (2019)[25], the latter marked with stars (\*). (G) Violin plots showing the expression of differentially expressed genes between young wt hair cells expressing Emx2 and young wt hair cells, in which Emx2 was not detected, adjusted p-value<0,01. (H) Fluorescent in situ hybridization of the same neuromasts as shown in Figure 1H, showing HCs in green, nuclei in blue (DAPI staining) and Emx2 in red (FISH) in 5 dpf wt and Emx2-mutant larvae. The scale bar is 10  $\mu$ m. (I) Immunohistochemical staining of the same neuromast as shown in Figure 1I, showing HCs in green, nuclei in blue (DAPI staining) and Emx2 in red (antibody staining) in wt and Emx2-mutant larvae. (J) Immunohistochemical staining of Emx2 in horizontal neuromasts in the transgenic line Tg[myo6b: actb1-EGFP] showing HCs in green, nuclei in blue (DAPI staining) and Emx2 in red (antibody staining) in 2dpf old wt and Atoh1a mutant larvae. wt n=24 (neuromasts), Atoh1a -/- n=10 (neuromasts). Scale bars are 10  $\mu$ m. (K) Fluorescent in situ hybridization of Emx2 in horizontal neuromast showing nuclei in blue (DAPI staining) and Emx2 in red (FISH) in 5 dpf old wt, Atoh1a mutant larvae. Scale bars are 10  $\mu$ m.

wt, wild type; HC, hair cell; dpf, days post fertilization; FISH, fluorescent in situ hybridization.

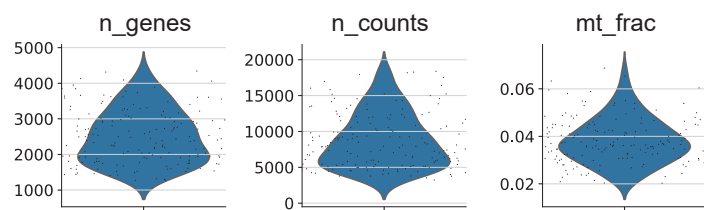
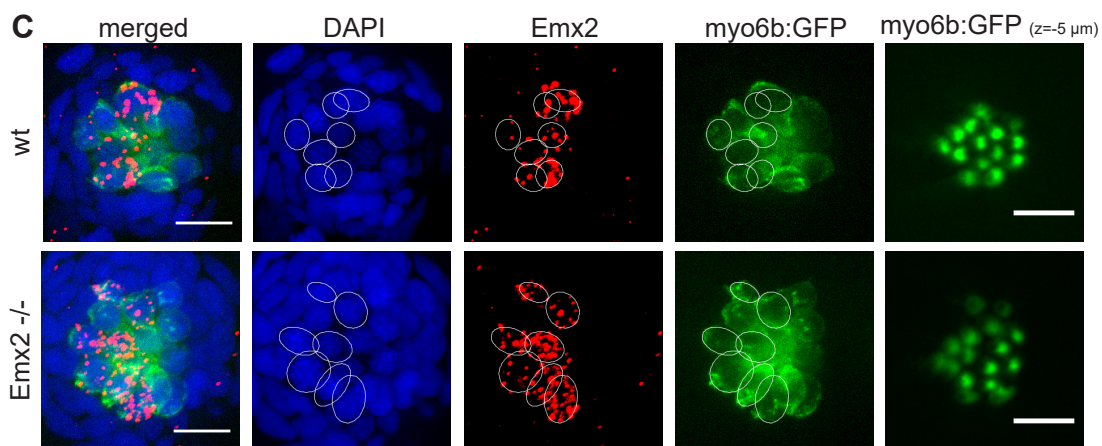
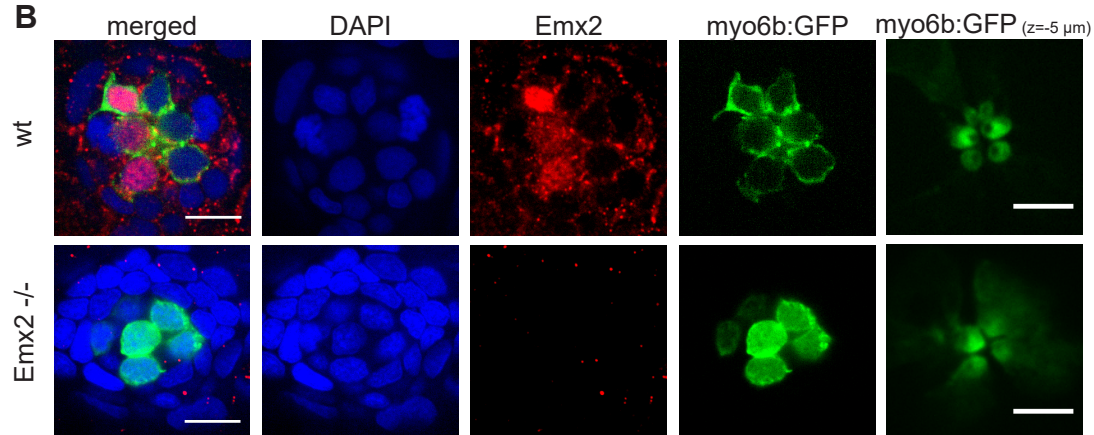
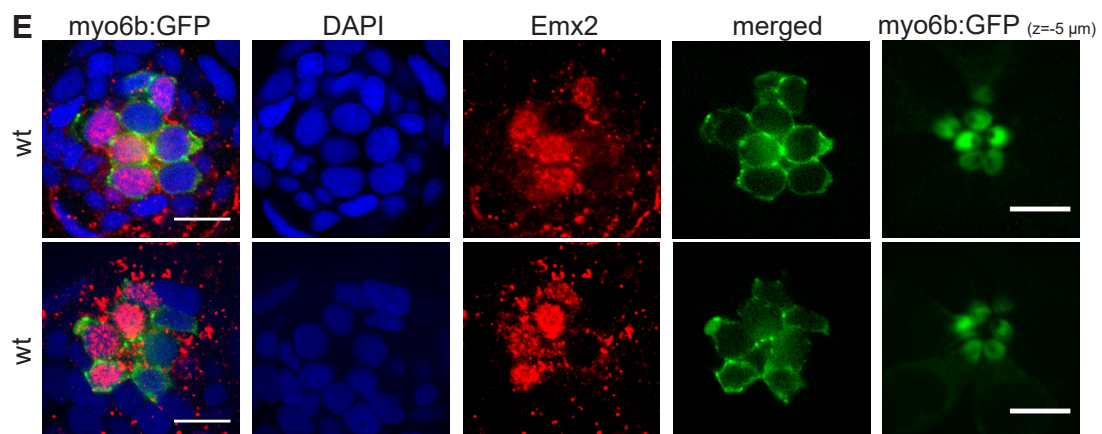
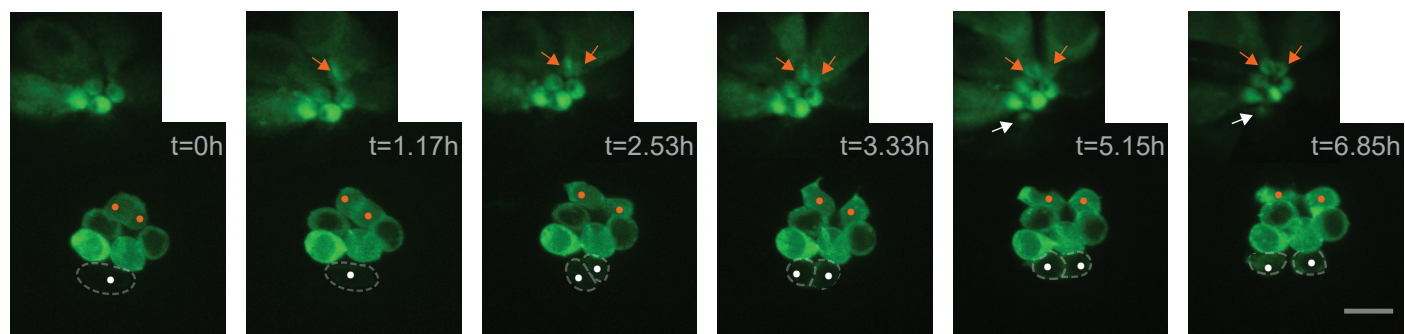




**Figure S3. Analysis of Emx2 expression in wild-type, Notch1a mutant, and Notch1a gain of function hair cells. Related to Figure 2.**

(A) Fluorescent in situ hybridization of the same neuromasts as shown in Figure 2D, showing HCs in green, nuclei in blue (DAPI staining) and Emx2 in red (FISH) in 5 dpf wt and Notch1a larvae. The scale bars are 10  $\mu$ m. (B) Immunohistochemical staining of the same neuromasts as shown in Figure 2C, showing HCs in green, nuclei in blue (DAPI staining) and Emx2 in red (antibody staining) in wt and Notch1a mutant larvae. The scale bars in the far right panel showing hair bundles are 5 $\mu$ m, in all other panels 10  $\mu$ m. (C) Immunohistochemical staining of the same neuromasts as shown in Figure 2J and 2N, showing HCs in green, nuclei in blue (DAPI staining) and Emx2 in red (antibody staining) in wt, DAPT-treated and Notch1a mutant, DAPT-treated larvae. The scale bars in the far right panel showing hair bundles are 5 $\mu$ m, in all other panels 10  $\mu$ m. (D) Immunohistochemical staining of the same neuromasts as shown in Figure 2L and the control wt neuromast, showing, nuclei in blue (DAPI staining) and Emx2 in red (antibody staining) and hair bundles in green (phalloidin staining) in wt and *brn3c:gal4, UAS:NICD* larvae. The scale bars in the far right panel showing hair bundles are 5  $\mu$ m, in all other panels 10  $\mu$ m.

wt, wild type; HC, hair cell; dpf, days post fertilization; FISH, fluorescent in situ hybridization.

**A****B****D**



**Figure S4. Analysis of Emx2 expression in wild-type and Emx2 mutant hair cells. Related to Figure 3.**

(A) Violin plots showing the three covariates used for preprocessing: number of detected genes (*n\_genes*), number of counts (*n\_counts*) and the fraction of counts from mitochondrial genes (*mt\_frac*) per barcode in the wt and Emx2-mutant samples after quality control sequenced by mcSCRBseq. (B) Immunohistochemical staining of the same neuromasts as shown in Figure 3B, showing HCs in green, nuclei in blue (DAPI staining) and Emx2 in red (antibody staining) in wt and Emx2-mutant larvae. (C) Fluorescent in situ hybridization of the same neuromasts as shown in Figure 3C, showing HCs in green, nuclei in blue (DAPI staining) and Emx2 in red (FISH) in 5 dpf wt and Emx2-mutant larvae. The scale bars in the far right panel showing hair bundles are 5µm, in all other panels 10 µm. (D) Selected images from a 6.85-hour time-series of a *myo6b*:EGFP horizontal neuromast with strongly green-fluorescent hair cells and a weakly fluorescent UHCP (white dot). After 2.53 hours, an UHCP divides into a pair of young hair cells, which mature during the following 4.32 hours (white dots). An earlier pair of hair cells is labeled with orange dots. The image series shows that green fluorescence in Tg[*myo6b*:*actb1*-EGFP] first appears in UHCPs. Additionally, the arrows in the top left images highlight the first stages of the formation of hair bundles in hair cells, which was used for the estimation of the immature hair cells age. The immature hair cells were defined as GFP-expressing cells, since the division of the UHCP until the kinocilium becomes visible (in *myo6b*:EGFP transgenic line), see far right panel. Scale bar is 10 µm, with 2x magnification in the additional top left images, showing hair bundles. (E) Immunohistochemical staining of the same neuromasts as shown in Figure 3D and 3E, showing HCs in green, nuclei in blue (DAPI staining) and Emx2 in red (antibody staining) in wt *myo6b*:EGFP larvae.

wt, wild type; UHCP, unipotent hair cell progenitor; dpf, days post fertilization; FISH, fluorescent in situ hybridization.